

Dinitrogen Difluoride Chemistry. Improved Syntheses of *cis*- and *trans*-N₂F₂, Synthesis and Characterization of N₂F⁺Sn₂F₉⁻, Ordered Crystal Structure of N₂F⁺Sb₂F₁₁⁻, High-Level Electronic Structure Calculations of *cis*-N₂F₂, *trans*-N₂F₂, F₂N=N, and N₂F⁺, and Mechanism of the *trans*–*cis* Isomerization of N₂F₂[†]

Karl O. Christe,^{*,§} David A. Dixon,[#] Daniel J. Grant,[#] Ralf Haiges,[§] Fook S. Tham,[⊥] Ashwani Vij,[‡] Vandana Vij,[‡] Tsang-Hsiu Wang,[#] and William W. Wilson[§]

[§]Loker Hydrocarbon Research Institute and Department of Chemistry, University of Southern California, Los Angeles, California 90089, [#]Department of Chemistry, University of Alabama, Tuscaloosa, Alabama 35487-0336, [⊥]Department of Chemistry, University of California, Riverside, California 92521, and [‡]Space and Missile Propulsion Division, Air Force Research Laboratory (AFRL/RZS), Edwards Air Force Base, California 93524

Received March 10, 2010

N₂F⁺ salts are important precursors in the synthesis of N₅⁺ compounds, and better methods are reported for their larger scale production. A new, marginally stable N₂F⁺ salt, N₂F⁺Sn₂F₉⁻, was prepared and characterized. An ordered crystal structure was obtained for N₂F⁺Sb₂F₁₁⁻, resulting in the first observation of individual N≡N and N–F bond distances for N₂F⁺ in the solid phase. The observed N≡N and N–F bond distances of 1.089(9) and 1.257(8) Å, respectively, are among the shortest experimentally observed N–N and N–F bonds. High-level electronic structure calculations at the CCSD(T) level with correlation-consistent basis sets extrapolated to the complete basis limit show that *cis*-N₂F₂ is more stable than *trans*-N₂F₂ by 1.4 kcal/mol at 298 K. The calculations also demonstrate that the lowest uncatalyzed pathway for the *trans*–*cis* isomerization of N₂F₂ has a barrier of 60 kcal/mol and involves rotation about the N=N double bond. This barrier is substantially higher than the energy required for the dissociation of N₂F₂ to N₂ and 2 F. Therefore, some of the N₂F₂ dissociates before undergoing an uncatalyzed isomerization, with some of the dissociation products probably catalyzing the isomerization. Furthermore, it is shown that the *trans*–*cis* isomerization of N₂F₂ is catalyzed by strong Lewis acids, involves a planar transition state of symmetry C_s, and yields a 9:1 equilibrium mixture of *cis*-N₂F₂ and *trans*-N₂F₂. Explanations are given for the increased reactivity of *cis*-N₂F₂ with Lewis acids and the exclusive formation of *cis*-N₂F₂ in the reaction of N₂F⁺ with F⁻. The geometry and vibrational frequencies of the F₂N=N isomer have also been calculated and imply strong contributions from ionic N₂F⁺ F⁻ resonance structures, similar to those in F₃NO and FNO.

Introduction

Polynitrogen compounds possess high energy and hold great potential as propellants and explosives.^{1,2} In 1999, the isolation of an exciting new polynitrogen compound, N₅⁺AsF₆⁻, was reported.¹ The synthesis of N₅⁺AsF₆⁻ and other N₅⁺ salts² was achieved by reacting N₂F⁺ salts with HN₃ in a suitable solvent. The following five-step process, originally used for generating the required N₂F⁺ salt (Scheme 1), was expensive and time-consuming and sometimes gave undesirable byproduct.

The synthesis of N₂F⁺ salts required the commercially unavailable N₂F₂. The latter can exist as both a *cis*- and a

trans-isomer, but only the *cis*-isomer reacts readily at ambient or subambient temperatures with strong Lewis acids to form the desired N₂F⁺ salts. Both isomers are planar, with C_{2v} symmetry for the *cis*- and C_{2h} symmetry for the *trans*-isomer. The *cis*-isomer has been reported to be thermodynamically slightly more stable than the *trans*-isomer.^{3,4} While most preparative methods for N₂F₂ result in mixtures of both isomers,³ its most convenient synthesis involving the reduction of N₂F₄ with graphite/AsF₅ intercalates⁵ produces only the less reactive *trans*-isomer, which must then be converted into the *cis*-isomer. Although *trans*–*cis* isomerization has been reported⁶ to occur

(3) For an exhaustive review of the properties and chemistry of N₂F₂ see: *Gmelin Handbook of Inorganic Chemistry, Fluorine*; Springer Verlag: Berlin, 1986; Suppl. Vol. 4, pp 385–403.

(4) Lee, T. J.; Rice, J. E.; Scuseria, G. E.; Schaefer, H. F., III. *Theor. Chim. Acta* **1989**, *75*, 81.

(5) Münch, V.; Selig, H. *J. Fluorine Chem.* **1980**, *15*, 235.

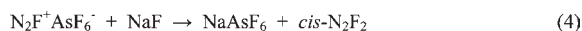
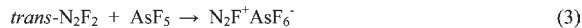
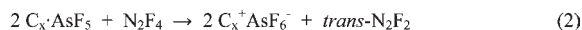
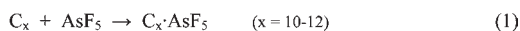
(6) Colburn, C. B.; Johnson, F. A.; Kennedy, A.; McCallum, K.; Metzger, L. C.; Parker, C. O. *J. Am. Chem. Soc.* **1959**, *81*, 6397.

[†] This paper is dedicated to the memory of Ira B. Goldberg.
*To whom correspondence should be addressed. E-mail: kchriste@usc.edu.

(1) Christe, K. O.; Wilson, W. W.; Sheehy, J. A.; Boatz, J. A. *Angew. Chem., Int. Ed.* **1999**, *38*, 2004.

(2) Christe, K. O. *Propellants, Explos., Pyrotechn.* **2007**, *32*, 194.

Scheme 1



above 225 °C in a copper flow tube, the uncatalyzed reaction has a very high activation energy barrier, with calculated values⁴ ranging from 65 to 85 kcal mol⁻¹. However at these temperatures, the thermal decomposition of N₂F₂ to NF₃, N₂, and F₂ proceeds quite readily. Therefore, the high-temperature gas phase isomerization must compete with the decomposition reaction, which might result in autocatalysis, and renders the isomerization reaction difficult to control. A reported experimental barrier⁷ of only 32 kcal mol⁻¹ for the gas phase isomerization reaction is suspect⁸ and needs verification. Isomerizations at temperatures below 225 °C involve long induction periods of weeks or months, consistent with the calculated high barriers and the possible need for creating first catalytically active metal fluoride surfaces by the reaction of some fluorine decomposition product with metal components. Therefore, finding convenient and reproducible isomerization conditions was important for scale-up reactions. In the past,^{1,9} this problem had been overcome by reacting *trans*-N₂F₂ with the strong Lewis acid AsF₅ under carefully controlled conditions, at 75 °C and elevated pressure, to give N₂F⁺AsF₆⁻. Subsequent displacement reactions of the resulting N₂F⁺AsF₆⁻ with a strong Lewis base, such as FNO or alkali metal fluorides in HF solution, resulted in the exclusive formation of *cis*-N₂F₂, thus providing a high-yield but cumbersome method for the synthesis of pure *cis*-N₂F₂, which then could be used for the synthesis of N₂F⁺ salts other than AsF₆⁻.

Further drawbacks of the previous process¹ were the use of expensive highly oriented pyrolytic graphite (HOPG) for preparing the AsF₅ intercalate and the need for long reaction times, stoichiometric amounts of AsF₅, and an extra step, the displacement reaction. In this paper experimental solutions are presented that mitigate these problems. Using high-level quantum chemical calculations, a better understanding of the underlying chemistry was also gained and some of the questions concerning the mechanism and thermodynamics of the N₂F₂ *trans*-*cis* isomerization⁹ were answered. With the crystal structure of N₂F⁺Sb₂F₁₁⁻, the first ordered structure of an N₂F⁺ salt was determined and the synthesis of the new N₂F⁺ salt, N₂F⁺Sn₂F₉⁻, is communicated. In addition, a theoretical study of the F₂N=N isomer was carried out, resulting in the prediction of an unusual structure with highly ionic N-F bonds, similar to those found in F₃NO¹⁰ and FNO.^{11,12}

(7) Binenboym, J.; Burcat, A.; Lifshitz, A.; Shamir, J. *J. Am. Chem. Soc.* **1966**, *88*, 5039.

(8) Slanina, Z. *Chem. Phys. Lett.* **1977**, *50*, 418.

(9) Christe, K. O.; Wilson, R. D.; Wilson, W. W.; Bau, R.; Sukumar, S.; Dixon, D. A. *J. Am. Chem. Soc.* **1991**, *113*, 3795.

(10) Christe, K. O.; Curtis, E. C.; Schack, C. J. *Spectrochim. Acta* **1975**, *31A*, 1035.

(11) Christe, K. O.; Guertin, J. P. *Inorg. Chem.* **1965**, *4*, 905.

(12) Holleman-Wiberg. *Inorganic Chemistry*; Academic Press: San Diego, CA, 2001; p 664.

Experimental Section

Caution! Some of the compounds used in this study are strong oxidizers, and anhydrous HF is corrosive and can cause severe burns on contact with skin. Recommended safety precautions include the wearing of face shields, leather gloves, and protective leather clothing.

Materials and Apparatus. Arsenic pentafluoride (Advance Research Chemicals) and N₂F₄ (Air Products) were purified by fractional condensation prior to use. Fluorine (Allied Chemical) was passed through a NaF scrubber for removal of HF, and antimony pentafluoride (Ozark Mahoning) was used as received. Powdered natural graphite flakes (Asbury Graphite Mills, No. 3243 50–60 μm) were treated with 360 Torr of fluorine gas to remove traces of moisture and reactive impurities before their intercalation with AsF₅. Hydrogen fluoride (Matheson Co.) was dried over BiF₅ as described earlier.¹³ Due to the corrosive and hazardous nature of the compounds used during this work, a stainless steel Teflon-FEP vacuum line, fitted with Hoke valves, was used.¹⁴ The vacuum line and all reaction vessels were passivated with ClF₃ prior to use. Pressures were measured with a Heise-Bourdon tube-type gauge (0–1500 mm ±0.1%). All nonvolatile materials were handled in the inert atmosphere of a glovebox.

Infrared spectra were recorded on a Mattson Galaxy FTIR spectrometer. The Raman spectra were measured either on a Cary model 83GT spectrometer using the 488 nm line of an Ar-ion laser or on a Bruker Equinox 55 spectrometer using the 1064 nm line of a Nd:YAG laser. The infrared spectra of gaseous samples were taken using a Monel IR cell equipped with a stainless steel valve and AgCl windows. The spectra of solid samples were recorded as powders pressed between AgCl or AgBr windows.

The single-crystal X-ray diffraction data were collected on a Bruker 3-circle platform diffractometer equipped with a SMART CCD (charge-coupled device) detector with the χ -axis fixed at 54.74° and using Mo K α radiation ($\lambda = 0.71073$ Å) from a fine-focus tube. This diffractometer was equipped with an LT-3 apparatus for low-temperature data collection using controlled liquid nitrogen boil off. Single crystals were selected in a glovebox, equipped with a CCD camera mounted microscope, and immersed in a culture slide's cavity containing PFPE (perfluoropolyether) oil. The culture slide was then taken out of the glovebox, and a suitable crystal was scooped out with a magnetic Cryoloop and mounted in a cold nitrogen stream on the magnetic goniometer head. Cell constants were determined from 90 30-s frames. A complete hemisphere of data was scanned on omega (0.3°) with a run time of 30 s per frame at a detector resolution of 512 × 512 pixels using the SMART software.¹⁵ A total of 1271 frames were collected in three sets. A final set of 50 frames, identical to the first 50 frames, was also collected to determine if any crystal decay had occurred. The frames were then processed on a PC by using the SAINT software¹⁶ to give the *hkl* file corrected for *Lp*/decay. The absorption correction was performed using the SADABS¹⁷ program. The structures were solved by the direct method using the SHELX-90¹⁸ program and refined by the least-squares method on F², SHELXL-97,¹⁹ incorporated in SHELXTL Suite

(13) Christe, K. O.; Wilson, W. W.; Schack, C. J. *J. Fluorine Chem.* **1978**, *11*, 71.

(14) Christe, K. O.; Wilson, R. D.; Schack, C. J. *Inorg. Synth.* **1986**, *24*, 3.

(15) SMART V 4.045, Software for the CCD Detector System; Bruker AXS: Madison, WI, 1999.

(16) SAINT V 4.035, Software for the CCD Detector System; Bruker AXS: Madison, WI, 1999.

(17) SADABS, Program for absorption correction for area detectors, Version 2.01; Bruker AXS: Madison, WI, 2000.

(18) Sheldrick, G. M. SHELXS-90, Program for the Solution of Crystal Structure; University of Göttingen: Germany, 1990.

(19) Sheldrick, G. M. SHELXL-97, Program for the Refinement of Crystal Structure; University of Göttingen: Germany, 1997.

5.10 for Windows NT.²⁰ All atoms were refined anisotropically. For the anisotropic displacement parameters, the $U(\text{eq})$ is defined as one-third of the trace of the orthogonalized U^{ij} tensor.

Intercalation of Graphite with AsF₅. Natural graphite flakes (120 g, 1 mol based on C₁₀) were loaded into a prepassivated 1 L Monel cylinder, which was then attached to a steel vacuum line and evacuated. Teflon filters were used to prevent any graphite powder from being blown into the line. About 25 mmol of fluorine gas was slowly bled into the evacuated cylinder. After keeping the cylinder for 12 h at room temperature, unreacted fluorine was pumped off and passed through a -196 °C trap followed by a soda-lime scrubber. The volatiles trapped at -196 °C consisted mainly of CO₂, CF₄, SiF₄, HF, and a trace of C₂F₆. Then, AsF₅ (173 g, 1.02 mol) was slowly bled at room temperature into the reactor, and a rapid pressure drop indicated the onset of intercalation. The total AsF₅ addition took about 2 h, after which the AsF₅ uptake became negligible. At this point, the cylinder was cooled to -196 °C and the remaining AsF₅ was condensed in. The cylinder was warmed to room temperature for ~72 h, after which time the volatiles were pumped off through a -196 °C trap. The contents of this trap consisted of small amounts of AsF₃, CF₄, and SiF₄ and showed only traces of AsF₅. The graphite showed a weight gain of 141 g (0.83 mol of AsF₅), indicative of a first-stage intercalate having the approximate composition C₁₂AsF₅. This intercalate was subsequently used to reduce the N₂F₄ to N₂F₂.

In a separate experiment, the cylinder was heated to 45 °C after condensing the AsF₅ onto the graphite. This resulted in a lower weight uptake and the generation of large amounts of AsF₃ along with other decomposition products. Therefore, heating must be avoided when carrying out the intercalation reaction.

Reduction of N₂F₄ with the Graphite Intercalate. This reaction was carried out as described by Selig,⁵ but the reaction time was reduced to ~38 h as opposed to ~5 days. In a typical experiment, 200 mmol of N₂F₄ was condensed at -196 °C into an evacuated 300 mL stainless steel reactor containing 138 mmol of C₁₂AsF₅. The cylinder was allowed to warm slowly to room temperature and kept at this temperature for 38 h. Noncondensable material, mainly nitrogen gas, was removed by evacuating the reactor at -196 °C. The room-temperature volatiles were fractionated through traps held at -156 and -196 °C. The -156 °C trap contained *trans*-N₂F₂ (194.5 mmol, ~97% yield based on N₂F₄), while the -196 °C trap contained some NF₃ and CF₄.

Isomerization Reactions of *trans*-N₂F₂. A reaction between *trans*-N₂F₂ (103 mmol) and SbF₅ (19.42 mmol) was carried out in a 100 mL Monel cylinder for 6 days at room temperature. The cylinder was then cooled to -196 °C and checked for any noncondensable material. None was detected. It was then kept in a -64 °C bath, and the volatiles were pumped through traps held at -156 and -196 °C. Nothing was trapped at -156 °C, and the -196 °C trap contained mainly *cis*-N₂F₂ (~75 mmol) and smaller amounts of *trans*-N₂F₂, NF₃, and CF₄. In the reactor, a white solid remained, consisting of N₂F⁺Sb₂F₁₁⁻ (~3.5 g).

In another experiment, a 30 mL passivated 316-stainless steel cylinder was loaded in the glovebox with AlF₃ (0.7 mmol) and attached to the vacuum line. The cylinder was evacuated and treated with 800 Torr of F₂ for 16 h at room temperature. After removal of the F₂, the cylinder was cooled to -196 °C and evacuated, and *trans*-N₂F₂ (12.1 mmol) was condensed in. The reactor was allowed to warm to room temperature and then heated in an oil bath to 55 °C for 16 h and cooled to room temperature. It was checked for any noncondensable material at -196 °C, but none was detected. The room-temperature

volatiles (12.0 mmol) were trapped at -196 °C and consisted of *cis*-N₂F₂ (90%), *trans*-N₂F₂ (10%), and a trace of NF₃.

When this experiment was repeated under identical conditions in a prepassivated 316-stainless steel reactor but in the absence of AlF₃, identical results (90% *cis*- and 10% *trans*-N₂F₂) were obtained.

However, when the experiment was scaled up to 40 mmol of *trans*-N₂F₂ in the same size 30 mL prepassivated 316-stainless steel cylinder, a strongly exothermic reaction occurred upon insertion into the oil bath at 55 °C, resulting in a sharp temperature rise and complete decomposition of the *trans*-N₂F₂ to NF₃, N₂, and F₂.

In a separate experiment, a 10 mL Teflon-FEP reactor, containing 30 mg of AlF₃, was loaded with *trans*-N₂F₂ (0.77 mmol) and heated to 55 °C for 16 h, resulting in a 90% conversion of *trans*-N₂F₂ to *cis*-N₂F₂.

In a similar experiment in a Teflon reactor but in the absence of AlF₃, no isomerization of *trans*-N₂F₂ was observed.

Preparation of N₂F⁺SbF₆⁻ and N₂F⁺Sb₂F₁₁⁻. In order to obtain well-defined stoichiometries, exact amounts of SbF₅ and *cis*-N₂F₂ were combined in anhydrous HF solution. For this purpose, a prepassivated Teflon ampule, equipped with a stainless steel Hoke valve and a Teflon-coated magnetic stirring bar, was loaded in the glovebox with SbF₅ (20.3 mmol), attached to the vacuum line, and evacuated at -196 °C. Anhydrous HF (~2 mL) was condensed into the ampule, and the reaction mixture was allowed to warm to ambient temperature to dissolve the SbF₅. The ampule was cooled to -196 °C, and a slight excess of *cis*-N₂F₂ (~22 mmol) was added. The ampule was allowed to warm slowly toward room temperature and then stirred vigorously for about 10 min. The volatiles were pumped off at -64 °C for 2 h until a constant weight was attained, leaving behind a white, free-flowing powder. The observed weight gain (5.71 g) corresponded to the formation of 20.2 mmol of N₂F⁺SbF₆⁻ (99.7% yield based on SbF₅).

The N₂F⁺Sb₂F₁₁⁻ salt was prepared in a similar manner by reacting 3.1 mmol of SbF₅ with 3.1 mmol of N₂F⁺SbF₆⁻ in ~2 mL of HF. N₂F⁺Sb₂F₁₁⁻ was obtained as a white, flaky solid in quantitative yield. The infrared and Raman spectra of these compounds agreed well with those reported in the literature.^{9,21–25}

Synthesis of N₂F⁺Sn₂F₉⁻. When anhydrous HF suspensions of SnF₄ were treated for several days at ambient temperature in either Teflon-FEP ampules or 316-stainless steel cylinders with a 2- to 4-fold molar excess of *cis*-N₂F₂, white solid residues were obtained upon removal of the volatile products. Based on the observed material balances, the combining ratios of SnF₄:*cis*-N₂F₂ were always very close to 2:1. The Raman and infrared spectra of these solids showed the presence of bands due to N₂F⁺ cations^{9,21–25} and tin fluoride anions.^{26–28} Therefore, the empirical composition of these solids is best described as N₂F⁺Sn₂F₉⁻. In one instance, a solid was obtained with a composition closer to 1:1, the vibrational spectra of which showed the presence of trapped *cis*-N₂F₂,²⁹ indicating that salts richer in N₂F⁺, such as N₂F⁺SnF₅⁻, are thermally unstable at room temperature and decompose with the evolution of *cis*-N₂F₂.

Crystal Structure Determination of N₂F⁺SbF₆⁻. Single crystals of N₂F⁺SbF₆⁻ were grown from HF solutions at -45 °C in a Teflon-FEP ampule. The solvent was slowly removed in a static

(21) Christie, K. O.; Wilson, R. D.; Sawodny, W. *J. Mol. Struct.* **1971**, *8*, 245.

(22) Ruff, J. K. *Inorg. Chem.* **1966**, *5*, 1971.

(23) Shamir, J.; Binenboym, J. *J. Mol. Struct.* **1969**, *4*, 100.

(24) Moy, D.; Young, A. R. *J. Am. Chem. Soc.* **1965**, *87*, 1889.

(25) Roesky, H. W.; Glemser, O.; Bormann, D. *Chem. Ber.* **1966**, *99*, 1589.

(26) Christie, K. O.; Schack, C. J. *Inorg. Chem.* **1978**, *17*, 2749.

(27) Christie, K. O.; Schack, C. J.; Wilson, R. D. *Inorg. Chem.* **1977**, *16*, 849.

(28) Wilson, W. W.; Vij, A.; Vij, V.; Bernhardt, E.; Christie, K. O. *Chem.—Eur. J.* **2003**, *9*, 2840.

(29) King, S. T.; Overend, J. *Spectrochim. Acta* **1967**, *23A*, 61.

(20) SHELXTL 5.10 for Windows NT, Program Library for Structure Solution and Molecular Graphics; Bruker AXS: Madison, WI, **1997**.

vacuum by condensation into a $-78\text{ }^{\circ}\text{C}$ trap. Suitable crystals were selected in the drybox and mounted as described in the Experimental Section. The diffraction data indicated no crystal decay during the data collection, but the nylon loop was charred when the mounted crystal was allowed to warm to room temperature. The intensity statistics and E -values did not provide an unambiguous choice of space groups in the orthorhombic crystal system. Systematic absences, i.e., absence of $h+k = \text{odd}$ reflections, however, clearly indicated a C -centered lattice. The structure could be solved in both centrosymmetric ($Cmmm$) and non-centrosymmetric space groups ($C222$ and $Amm2$). The $Cmmm$ and $C222$ space groups placed the central nitrogen atom, bonded to one other atom, nitrogen or fluorine, of the N_2F^+ cation on a mirror plane, thereby generating disorder in the $\text{N}-\text{N}-\text{F}$ bonds. The structure was refined with nitrogen and fluorine atoms on the same sites with equal occupancy factors. This model failed to give the individual $\text{N}-\text{N}$ and $\text{N}-\text{F}$ bond distances and, therefore, provided information only on the $r_{\text{N}=\text{N}} + r_{\text{N}-\text{F}}$ distances. Both these space groups refined the structure to the same R -value of 3.9%, and similar structural parameters were obtained. The final choice of $Cmmm$ being the correct space group was made on the basis that it has higher symmetry and only half of the parameters needed to be refined. An alternate choice of the $Amm2$ space group was rejected although it allowed the determination of individual $\text{N}-\text{N}$ and $\text{N}-\text{F}$ bonds, because the atoms did not have good thermal values and the R -value was considerably higher.

Crystal Structure Determination of $\text{N}_2\text{F}^+\text{Sb}_2\text{F}_{11}^-$. The $\text{N}_2\text{F}^+\text{Sb}_2\text{F}_{11}^-$ crystals obtained from the reaction of *trans*- N_2F_2 with SbF_5 at room temperature were used for this diffraction study. A suitable single crystal was mounted using a CryoLoop as described above. The intensity statistics, i.e., $E^2 - 1$ values, indicated a centrosymmetric space group for $\text{N}_2\text{F}^+\text{Sb}_2\text{F}_{11}^-$. Furthermore, the absence of $0k0$ ($k = \text{odd}$) and $h0l$ reflections ($h+l = \text{odd}$) showed the presence of a 2_1 screw axis and an n -glide plane parallel and perpendicular to the b -axis, respectively. The space group was thus unambiguously assigned as $P2_1/n$.

Computational Methods. The computational approach developed at The University of Alabama and Washington State University for the prediction of accurate molecular thermochemistry was used to predict the heats of formation and important energetic features of these compounds.^{30–32} The approach is based on calculating the total atomization energy of a molecule and using this value with known heats of formation of the atoms to calculate the heat of formation at 0 K. The approach starts with coupled cluster theory with single and double excitations and includes a perturbative triples correction (CCSD(T)),^{33–35} combined with the correlation-consistent basis sets³⁶ extrapolated to the complete basis set (CBS) limit to treat the correlation energy of the valence electrons. This is followed by a number of smaller additive corrections including core–valence interactions and relativistic effects, both scalar and spin–orbit. The zero-point energy can be obtained from experiment, theory, or a combination of the two. Corrections to 298 K can then be calculated by using standard thermodynamic

and statistical mechanics expressions in the rigid rotor-harmonic oscillator approximation³⁷ and appropriate corrections for the heat of formation of the atoms.³⁸

The standard aug-cc-pVnZ basis sets were used for N and F and abbreviated as aVnZ. Only the spherical component subsets (e.g., five-term d functions, seven-term f functions, etc.) of the Cartesian polarization functions were used. All CCSD(T) calculations were performed with the MOLPRO-2002 program system³⁹ on an SGI Altix computer, the Cray XD-1, the dense memory Linux cluster at the Alabama Supercomputer Center, or the Dell Linux cluster at The University of Alabama. For the open-shell atomic calculations, the restricted method for the starting Hartree–Fock wave function was used, and then the spin restriction in the coupled cluster portion of the calculation was relaxed. This method is conventionally labeled R/UCCSD(T).^{40–42}

The geometries were optimized at the CCSD(T) level with the aVDZ and aVTZ basis sets except for N_2F , where only the aVDZ geometry was obtained. The aVTZ geometries were then used in single-point CCSD(T)/aVQZ calculations. The zero-point energies (ΔE_{ZPE}) were calculated at the CCSD(T)/aVTZ level without scaling. For the CBS estimates, a mixed exponential/Gaussian function of the form⁴³

$$E(n) = E_{\text{CBS}} + \text{Be}^{-(n-1)} + \text{Ce}^{-(n-1)^2} \quad (6)$$

was used, where $n = 2$ (aVDZ), 3 (aVTZ), and 4 (aVQZ). Core–valence (CV) calculations were carried out at the CCSD(T) level with the weighted CV basis set cc-pwCVTZ.⁴⁴ The atomic spin–orbit corrections are $\Delta E_{\text{SO}}(\text{O}) = 0.22$, $\Delta E_{\text{SO}}(\text{F}) = 0.39$, and $\Delta E_{\text{SO}}(\text{F}^+) = 0.48$ kcal/mol, taken from the tables of Moore.⁴⁵ ΔE_{SR} was evaluated by using expectation values for the two dominant terms in the Breit–Pauli Hamiltonian, the so-called mass-velocity and one-electron Darwin (MVD) corrections from configuration interaction singles and doubles (CISD) calculations⁴⁶ with the aVTZ basis set at the appropriate optimized geometry. By combining the computed $\sum D_0$ values, given by the following expression,

$$\sum D_0 = \sum E_{\text{elec}}(\text{CBS}) - \Delta E_{\text{ZPE}} + \Delta E_{\text{CV}} + \Delta E_{\text{SR}} + \Delta E_{\text{SO}} \quad (7)$$

with the known heats of formation at 0 K for the elements, the $\Delta H_{f,0\text{K}}$ values can be derived. The heats of formation of N and F are $\Delta H_{f,0\text{K}}(\text{N}) = 112.53$ kcal/mol and $\Delta H_{f,0\text{K}}(\text{F}) = 18.47$ kcal/mol.⁴⁷

(37) McQuarrie, D. A. *Statistical Mechanics*; University Science Books: Sausalito, CA, 2001.

(38) Curtiss, L. A.; Raghavachari, K.; Redfern, P. C.; Pople, J. A. *J. Chem. Phys.* **1997**, *106*, 1063.

(39) Amos, R. D.; Bernhardsson, A.; Berning, A.; Celani, P.; Cooper, D. L.; Deegan, M. J. O.; Dobbyn, A. J.; Eckert, F.; Hampel, C.; Hetzer, G.; Knowles, P. J.; Korona, T.; Lindh, R.; Lloyd, A. W.; McNicholas, S. J.; Manby, F. R.; Meyer, W.; Mura, M. E.; Nicklass, A.; Palmieri, P.; Pitzer, R.; Rauhut, G.; Schütz, M.; Schumann, U.; Stoll, H.; Stone, A. J.; Tarroni, R.; Thorsteinsson, T.; Werner, H.-J. *MOLPRO*, a package of *ab initio* programs, version 2006; Universität Stuttgart, Stuttgart, Germany, University of Birmingham, Birmingham, U.K., 2006.

(40) Rittby, M.; Bartlett, R. J. *J. Phys. Chem.* **1988**, *92*, 3033.

(41) Knowles, P. J.; Hampel, C.; Werner, H.-J. *J. Chem. Phys.* **1994**, *99*, 5219.

(42) Deegan, M. J. O.; Knowles, P. J. *Chem. Phys. Lett.* **1994**, *227*, 321.

(43) Peterson, K. A.; Woon, D. E.; Dunning, T. H., Jr. *J. Chem. Phys.* **1994**, *100*, 7410.

(44) Peterson, K. A.; Dunning, T. H., Jr. *J. Chem. Phys.* **2002**, *117*, 10548.

(45) Moore, C. E. *Atomic energy levels as derived from the analysis of optical spectra, Vol. 1, H to V*; U.S. National Bureau of Standards Circular 467, U.S. Department of Commerce, National Technical Information Service, COM-72-50282, Washington, D.C., 1949.

(46) Davidson, E. R.; Ishikawa, Y.; Malli, G. L. *Chem. Phys. Lett.* **1981**, *84*, 226.

(47) Chase, M. W., Jr. NIST-JANAF Tables, 4th ed. *J. Phys. Chem. Ref. Data* **1998**, Monogr. 9, Suppl. 1.

(30) Feller, D.; Peterson, K. A.; Dixon, D. A. *J. Phys. Chem. A* **2010**, *114*, 613.

(31) Feller, D.; Peterson, K. A.; Dixon, D. A. *J. Chem. Phys.* **2008**, *129*, 204105.

(32) Feller, D.; Dixon, D. A. *J. Phys. Chem. A* **2003**, *107*, 9641.

(33) Purvis, G. D., III; Bartlett, R. J. *J. Chem. Phys.* **1982**, *76*, 1910.

(34) Raghavachari, K.; Trucks, G. W.; Pople, J. A.; Head-Gordon, M. *Chem. Phys. Lett.* **1989**, *157*, 479.

(35) Watts, J. D.; Gauss, J.; Bartlett, R. J. *J. Chem. Phys.* **1993**, *98*, 8718.

(36) (a) Dunning, T. H., Jr. *J. Chem. Phys.* **1989**, *90*, 1007. (b) Kendall, R. A.; Dunning, T. H., Jr.; Harrison, R. J. *J. Chem. Phys.* **1992**, *96*, 6796. (c) Woon, D. E.; Dunning, T. H., Jr. *J. Chem. Phys.* **1993**, *98*, 1358. (d) Dunning, T. H., Jr.; Peterson, K. A.; Wilson, A. K. *J. Chem. Phys.* **2001**, *114*, 9244. (e) Wilson, A. K.; Woon, D. E.; Peterson, K. A.; Dunning, T. H., Jr. *J. Chem. Phys.* **1999**, *110*, 7667.

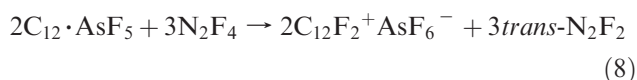
Heats of formation at 298 K were obtained by following the procedures outlined by Curtiss et al.³⁸

Results and Discussion

Preparation of the Graphite·AsF₅ Intercalate. The first step in the generation of N₂F⁺ salts is the formation of a first-stage intercalate of AsF₅ in graphite (eq 1). If highly oriented pyrolytic graphite (HOPG) is used, the intercalation is sluggish and requires several weeks to go to completion. Not only is HOPG very expensive, it is also difficult to grind. Replacing the HOPG graphite with finely powdered natural flake graphite (particle size of 50–60 μm), which is commercially available for about one dollar per pound, proved to be a highly efficient and economical method for preparing the required intercalate. In all the intercalation experiments performed during this work, the graphite powder was pretreated with small amounts of ambient pressure F₂ gas to remove impurities and traces of moisture. The major volatile products observed during this treatment were CF₄ and SiF₄. In different runs of the intercalation reaction, carried out at room temperature with reaction times of 2–3 days, the composition of the first-stage intercalate based on AsF₅ uptake corresponded to C_xAsF₅ (x = 10.4–12.0). Furthermore, it was found that mild warming of the reaction cylinder to ~40 °C accelerated the intercalation, but also resulted in the formation of significant amounts of CF₄ and AsF₃ due to the oxidation of the graphite by AsF₅. Therefore, heating of the cylinder to accelerate the intercalation rate should be avoided. As reported earlier, AsF₃ does not form a stable intercalate with graphite.⁵

Synthesis of *trans*-N₂F₂. Our method for the preparation of *trans*-N₂F₂ was based on the work of Münch and Selig⁵ and involved the reduction of N₂F₄ with a graphite/AsF₅ intercalate (eq 2). Without careful temperature control, varying amounts of N₂, F₂, and NF₃ were obtained with traces of SiF₄ and CF₄ as byproduct. However, addition of N₂F₄ at –196 °C, followed by slow and controlled warmup and use of the small particle size, natural flake graphite intercalate, resulted in a fast and quantitative reduction of the N₂F₄ to *trans*-N₂F₂ without formation of NF₃, N₂, and F₂. The quantitative formation of *trans*-N₂F₂ also eliminated its difficult separation from unreacted N₂F₄. No *cis*-N₂F₂ was observed in all of these reactions.

Münch and Selig reported⁵ that the reaction of first-stage graphite/AsF₅ intercalate with N₂F₄ was complete after one mole of N₂F₄ was converted per mole of intercalated AsF₅. The stoichiometry of this reaction was examined by adding the N₂F₄ in increments to the first-stage intercalate and analyzing the products after each N₂F₄ addition. Contrary to the report by Münch and Selig,⁵ it was found that 1 mol of intercalate was able to quantitatively reduce somewhat more than 1.5 mol of N₂F₄ to *trans*-N₂F₂. This demonstrates that eq 2 is a poor description of this reaction and that the graphite structure is also being fluorinated (eq 8).



Reaction of N₂F₂ with Lewis Acids and Its *trans*–*cis* Isomerization. In the previous study,⁹ excess *trans*-N₂F₂

was reacted with AsF₅ at 70 °C for 3 days to give yields of N₂F⁺AsF₆[–] of about 80% (eq 3). In this study, it was found that by cutting the reaction time in half, the yield of N₂F⁺AsF₆[–] could be increased to >99%, based on the amounts of AsF₅ used, and the decomposition of N₂F₂ to NF₃, N₂, and F₂ was suppressed. By adding the required amount of NaF to the cylinder containing the N₂F⁺AsF₆[–], condensing in HF, and shaking it vigorously at room temperature, quantitative yields of *cis*-N₂F₂ were obtained (eq 4), which then could be converted readily to other N₂F⁺ salts, such as N₂F⁺SbF₆[–], by reaction with the corresponding Lewis acid (eq 5).

When either N₂F⁺Sb₂F₁₁[–] is the desired product or the loss of some N₂F₂ in the form of N₂F⁺Sb₂F₁₁[–] can be tolerated, steps (3) and (4) can be greatly simplified by replacing the stoichiometric amount of AsF₅ required for (3) by catalytic amounts of SbF₅, thus avoiding the use of large amounts of expensive AsF₅ and eliminating the need for heating and for the displacement step (4). Thus, when *trans*-N₂F₂ was reacted for 6 days at room temperature with catalytic amounts of SbF₅, the 9:1 *cis*–*trans*-N₂F₂ equilibrium was established, while the catalytic amount of SbF₅ was converted to N₂F⁺Sb₂F₁₁[–] (eq 9). The N₂F⁺Sb₂F₁₁[–] was characterized by vibrational spectroscopy and its crystal structure (see below).



The most effective catalysts, however, were found to be either 10–20 mol % of commercial AlF₃, which had been pretreated with elemental F₂ gas at 60 °C, or the surfaces of 316-stainless steel cylinders, which had been passivated with strong fluorinating agents, such as F₂ or ClF₃. Running these isomerization reactions at 55 °C for 15 h, the limiting thermodynamic *cis*–*trans* equilibrium^{3,48} of 9:1 could successfully be reached. Examination of the used AlF₃ catalyst by Raman spectroscopy at room temperature showed no evidence for the presence of N₂F⁺ salts or retention of N₂F₂ by AlF₃. Furthermore, the catalyst was reusable and not consumed. It was also demonstrated that heating alone in the absence of a catalyst, i.e., using an all-Teflon reactor under the same conditions, did not result in isomerization.

Since N₂F₂ is thermodynamically unstable with respect to its decomposition products NF₃, N₂, and F₂,³ and stainless steel is a relatively poor thermal conductor, heating of steel cylinders, overloaded with N₂F₂, can lead to exothermic, uncontrolled thermal decomposition of the N₂F₂. Such an event was observed when a 30 mL pre-passivated stainless steel reactor, loaded with 40 mmol of *trans*-N₂F₂, was immersed into a 55 °C oil bath, resulting in a runaway exothermic decomposition reaction of all the N₂F₂ present. In a second case, a similarly overloaded reactor, but this time in the presence of catalytic amounts of SbF₅, also underwent N₂F₂ decomposition. The generated heat and pressure were sufficient to effect the reaction of SbF₅ with the NF₃ and F₂ decomposition products to yield NF₄⁺Sb₃F₁₆[–] according to eq 10.⁴⁹



(48) Pankratov, A. V.; Sokolov, O. M. *Russ. J. Inorg. Chem.* **1966**, *11*, 943.

(49) Christe, K. O.; Schack, C. J.; Wilson, R. D. *J. Fluorine Chem.* **1976**, *8*, 541.

It should be noted that the catalytic effect of prepassivated steel on the isomerization of N_2F_2 had already been mentioned more than 40 years ago,^{48,50} but has been widely ignored in subsequent work.

Structural Investigations of $N_2F^+SbF_6^-$ and $N_2F^+Sb_2F_{11}^-$. The N_2F^+ cation has been the subject of various spectroscopic, structural, and theoretical investigations.^{3,9,21–24,51–57} The most interesting features are the unusually short N–N and N–F bond lengths of 1.1034(5) and 1.2461(10) Å, respectively, observed by Botschwina et al. for the free gaseous ion using millimeter-wave spectroscopy.⁵² The shortest experimentally observed N–N bond distance is 1.09277(9) Å in N_2H^+ .⁵⁸ Christe et al. have previously determined the crystal structure of $N_2F^+AsF_6^-$.⁹ The compound crystallized in the centrosymmetric space group $C2m$ where the $N\equiv N$ and N–F bonds were disordered, and it was not possible to measure the bond lengths of each bond individually. The same disorder problem affects the crystal structure of $N_2F^+SbF_6^-$ in the present study, and only the sum of the N–N and N–F bond distances (2.340(9) Å) can be determined. Details on the disordered $N_2F^+SbF_6^-$ structure are given in the Supporting Information.

The crystal structure of $N_2F^+Sb_2F_{11}^-$ (Tables 1, 2, and S4) is ordered and allows the determination of the individual N–N and N–F bond lengths. This structure can be considered a true representation of the N_2F^+ cation in the solid state, and the linearity of the N–N–F bond is not automatically generated by symmetry as in the case of the $N_2F^+MF_6^-$ (M = As or Sb) salts. The structure (Figure 1) was solved in the $P2_1/n$ space group, and all of the atoms showed excellent thermal behavior. A final R value of 3.76% was obtained with no appreciable residual electron density left over, which would indicate some disorder. The sum of the N–N and N–F bond distances of 2.346(9) Å (Table 3) is in excellent agreement with the observed spectroscopic gas phase value of 2.3495 Å.⁵² In $N_2F^+Sb_2F_{11}^-$, the N–F distance of 1.257(8) Å is somewhat longer and the N–N distance of 1.089(9) Å is slightly shorter than those (1.2461 and 1.1034 Å, respectively) of gaseous N_2F^+ .⁵² The $N\equiv N$ distance in $N_2F^+Sb_2F_{11}^-$ can, therefore, be considered to be among the shortest, if not the shortest, experimentally observed N–N bond lengths. For comparison, the $N\equiv N$ bond distances in N_2 and HN_2^+ are 1.0976(2) and 1.09277(9) Å, respectively.^{58,59}

Figure S3 depicts the packing diagram of $N_2F^+Sb_2F_{11}^-$. The N_2F^+ cation lies between the Sb–F–Sb bend of the $Sb_2F_{11}^-$ anion at an angle of 68.4° with respect to the mean plane containing the F6–Sb1–F7–Sb2–F12 atoms. As in the case of $N_2F^+SbF_6^-$, no close contacts are found to and from the N_2F^+ cation.

Table 1. Crystal Data and Structure Refinement for $N_2F^+Sb_2F_{11}^-$

chemical formula	F12 N2 Sb2
fw	499.52
temp (°C)	–35 (2)
space group	$P2_1/n$
unit cell dimens	
a (Å)	7.558(2)
b (Å)	9.926(2)
c (Å)	14.103(2)
β (deg)	99.59(1)
volume (Å ³)	1043.2(4)
Z	4
D_{calc} (g/cm ³)	3.181
absorb coeff (cm ^{–1})	0.5329
final R indices [$I > 2\sigma(I)$]	$R_1^a = 0.0376$ $wR_2^b = 0.0895$
R indices (all data)	$R_1 = 0.0388$ $wR_2 = 0.0903$

$$^a R_1 = \frac{\sum ||F_o| - |F_c||}{\sum |F_o|}, ^b wR_2 = \left\{ \frac{\sum [w(F_o^2 - F_c^2)^2]}{\sum [w(F_o^2)^2]} \right\}^{1/2}.$$

The geometry of the $Sb_2F_{11}^-$ anion also deserves a special comment. The Sb–F–Sb bridge is bent with an angle of 145.2(2)° and coplanar with the terminal fluorines, F6 and F12, which are eclipsed. The equatorial fluorine atoms of each SbF_5 group are staggered with a twist angle of ~31° (Figure 2). The large variation in the structures of $Sb_2F_{11}^-$ anions in different compounds is due to its ease of deformation by crystal-packing effects.^{60,61}

Synthesis and Properties of $N_2F^+Sn_2F_9^-$. The only room-temperature-stable N_2F^+ salts, previously reported, were those derived from AsF_5 and SbF_5 , while BF_3 and PF_5 do not form stable N_2F^+ salts.^{3,9} Since SnF_4 , with a pF^- value of 9.8,^{62,63} is a stronger Lewis acid than either BF_3 or PF_5 and can form stable $N_2F_3^+$ and NF_4^+ salts,^{26,27} it was interesting to explore the interaction between SnF_4 and cis - N_2F_2 . Because SnF_4 is a highly polymeric solid, the reactions were carried out in anhydrous HF solution. It was found that SnF_4 reacts with excess cis - N_2F_2 in a 2:1 mol ratio, giving white solids with the empirical composition $N_2F^+Sn_2F_9^-$ (eq 11).



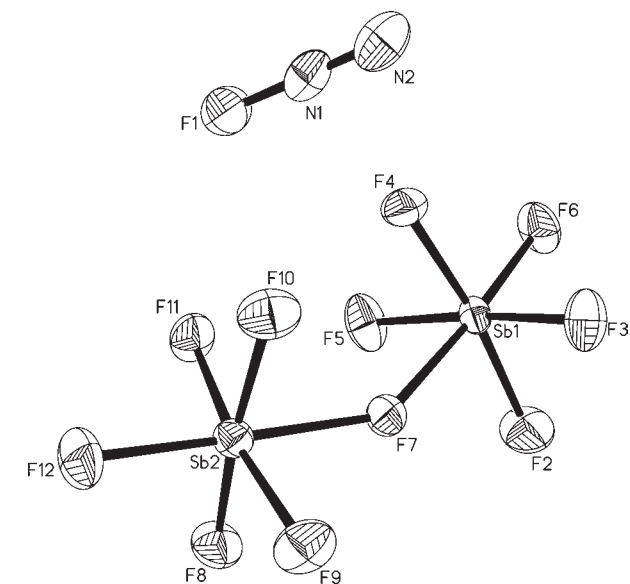
The products were characterized by vibrational spectroscopy (Figure S4, Table 4). They showed the three characteristic N_2F^+ bands and other bands of variable intensities in the regions characteristic for Sn(IV) fluoride anions,^{26–28} indicating the presence of polyanions of variable composition and structure. The N_2F^+ bands also showed some splittings of variable intensities indicative of the presence of more than one form of the counterion. A similar observation for the existence of polymeric tin fluoride anions of different composition has previously been made in our study of $N_5^+SnF_5^-$, where the “ SnF_5^- ” anion was shown²⁸ by multinuclear NMR spectroscopy to be present as a mixture of $Sn_2F_{10}^{2-}$ and $Sn_4F_{20}^{4-}$.

- (50) Lustig, M. *Inorg. Chem.* **1965**, *4*, 104.
 (51) Pankratov, A. V.; Savenkova, N. I. *Zh. Neorg. Khim.* **1968**, *13*, 2610.
 (52) Botschwina, P.; Sebald, P.; Bogey, M.; Demuyne, C.; Destombes, J. L. *J. Mol. Spectrosc.* **1992**, *153*, 255.
 (53) Mason, J.; Christe, K. O. *Inorg. Chem.* **1983**, *22*, 1849.
 (54) Glaser, R.; Choy, G. S. C. *J. Am. Chem. Soc.* **1993**, *115*, 2340.
 (55) Cacace, F.; Grandinetti, F.; Pepi, F. *Inorg. Chem.* **1995**, *34*, 1325.
 (56) Pulay, P.; Ruoff, A.; Sawodny, W. *Mol. Phys.* **1975**, *30*, 1123.
 (57) Peters, N. J. S. *Chem. Phys. Lett.* **1987**, *142*, 76.
 (58) Owrutsky, J. C.; Gudeman, C. S.; Martner, C. C.; Tack, L. M.; Rosenbaum, N. H.; Saykally, R. J. *J. Chem. Phys.* **1986**, *84*, 605.
 (59) Huber, K. P.; Herzberg, G. *Constants of Diatomic Molecules*; Van Nostrand Reinhold: New York, 1979.

- (60) Willner, H.; Bodenbinder, M.; Broechler, R.; Hwang, G.; Rettig, S. J.; Trotter, J.; von Ahsen, B.; Westphal, U.; Jonas, V.; Thiel, W.; Aubke, F. *J. Am. Chem. Soc.* **2001**, *123*, 588.
 (61) Vij, A.; Wilson, W. W.; Vij, V.; Tham, F. S.; Sheehy, J. A.; Christe, K. O. *J. Am. Chem. Soc.* **2001**, *123*, 6308.
 (62) Christe, K. O.; Dixon, D. A.; McLemore, D.; Wilson, W. W.; Sheehy, J. A.; Boatz, J. A. *J. Fluorine Chem.* **2000**, *101*, 151.
 (63) Christe, K. O.; Dixon, D. A. Paper 577, IN 3, presented at the 92nd Canadian Chemistry Conference, May 30, 2009, Hamilton, ON, Canada.

Table 2. Bond Lengths and Angles for $\text{N}_2\text{F}^+\text{Sb}_2\text{F}_{11}^-$

Bond Lengths (Å)			
Sb(1)–F(3)	1.868(4)	Sb(2)–F(8)	1.876(4)
Sb(1)–F(2)	1.873(4)	Sb(2)–F(11)	1.883(4)
Sb(1)–F(6)	1.879(4)	Sb(2)–F(10)	1.885(4)
Sb(1)–F(5)	1.887(4)	Sb(2)–F(12)	1.901(4)
Sb(1)–F(4)	1.894(4)	Sb(2)–F(7)	2.076(4)
Sb(1)–F(7)	2.077(4)	F(1)–N(1)	1.257(8)
Sb(2)–F(9)	1.865(4)	N(1)–N(2)	1.089(9)
Bond Angles (deg)			
N(2)–N(1)–F(1)	179.2(7)	F(8)–Sb(2)–F(7)–Sb(1)	114.5(4)
F(3)–Sb(1)–F(2)	89.6(2)	F(9)–Sb(2)–F(7)	85.64(18)
F(3)–Sb(1)–F(6)	95.9(2)	Sb(2)–F(7)–Sb(1)	145.2(2)
F(2)–Sb(1)–F(6)	95.2(2)	F(8)–Sb(2)–F(7)	86.46(18)
F(3)–Sb(1)–F(5)	172.1(2)	F(11)–Sb(2)–F(7)	84.74(17)
F(2)–Sb(1)–F(5)	89.8(2)	F(10)–Sb(2)–F(7)	86.6(2)
F(6)–Sb(1)–F(5)	92.0(2)	F(12)–Sb(2)–F(7)	178.61(18)
F(3)–Sb(1)–F(4)	90.8(2)	F(9)–Sb(2)–F(8)	90.5(2)
F(2)–Sb(1)–F(4)	170.3(2)	F(9)–Sb(2)–F(11)	170.39(19)
F(6)–Sb(1)–F(4)	94.4(2)	F(8)–Sb(2)–F(11)	89.0(2)
F(5)–Sb(1)–F(4)	88.5(2)	F(9)–Sb(2)–F(10)	90.4(2)
F(3)–Sb(1)–F(7)	87.56(18)	F(8)–Sb(2)–F(10)	172.9(2)
F(2)–Sb(1)–F(7)	87.55(19)	F(11)–Sb(2)–F(10)	88.9(2)
F(6)–Sb(1)–F(7)	175.64(17)	F(9)–Sb(2)–F(12)	95.7(2)
F(5)–Sb(1)–F(7)	84.56(18)	F(8)–Sb(2)–F(12)	93.5(2)
F(4)–Sb(1)–F(7)	82.80(17)	F(11)–Sb(2)–F(12)	93.86(19)
		F(10)–Sb(2)–F(12)	93.4(2)
Torsion Angles (deg)			
F(9)–Sb(2)–F(7)–Sb(1)	–154.8(4)	F(10)–Sb(2)–F(7)–Sb(1)	–64.1(4)
F(11)–Sb(2)–F(7)–Sb(1)	25.1(4)	F(12)–Sb(2)–F(7)–Sb(1)	26(8)
F(6)–Sb(1)–F(7)–Sb(2)	–19(3)	F(3)–Sb(1)–F(7)–Sb(2)	123.3(4)
F(5)–Sb(1)–F(7)–Sb(2)	–56.9(4)	F(2)–Sb(1)–F(7)–Sb(2)	–147.0(4)
F(4)–Sb(1)–F(7)–Sb(2)	32.2(4)		

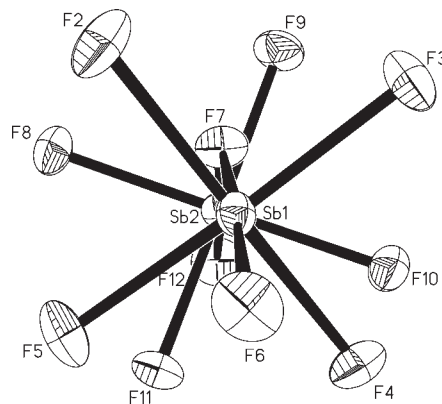
**Figure 1.** ORTEP plot for $\text{N}_2\text{F}^+\text{Sb}_2\text{F}_{11}^-$ with thermal ellipsoids at the 30% probability level.

The preferred formation of Sn_2F_9^- can be explained by the fact that monomeric SnF_4 is a weaker Lewis acid than its oligomers, in accord with our general finding that oligomeric Lewis acids are stronger acids than their monomers.^{62,63} Therefore, Sn_2F_9^- salts are more stable than SnF_5^- salts, which in turn are more stable than SnF_6^{2-} salts. This was also demonstrated when metathetical reactions between

Table 3. Calculated and Experimental Bond Distances (Å) for N_2F^+

molecule	method	$r_{\text{N}=\text{N}}$	$r_{\text{N}-\text{F}}$	$\sum(r_{\text{N}=\text{N}} + r_{\text{N}-\text{F}})$
$\text{N}_2\text{F}^+\text{AsF}_6^-$	X-ray ⁹	(1.099) ^a	(1.217) ^a	2.316(12)
$\text{N}_2\text{F}^+\text{SbF}_6^-$	X-ray ⁹	(1.110) ^a	(1.230) ^a	2.340(9)
$\text{N}_2\text{F}^+\text{Sb}_2\text{F}_{11}^-$	X-ray (this work)	1.089(9)	1.257(8)	2.346(9)
N_2F^+ (gas)	millimeter spectroscopy ⁴⁹	1.1034	1.2461	2.3495
N_2F^+ (gas)	CCSD(T)/aVTZ	1.1246	1.2357	2.360
N_2F^+ (gas)	CEPA-1/[8,4,2,1] ⁴⁹	1.1040	1.2521	2.3561

^a Obtained by partitioning the experimentally observed sum in the same ratio as that calculated at the LDFS2 level.

**Figure 2.** ORTEP plot showing the geometry of the $\text{Sb}_2\text{F}_{11}^-$ anion.

$\text{N}_2\text{F}^+\text{SbF}_6^-$ and either CsSnF_5 , Cs_2SnF_6 , or Na_2SnF_6 in HF solution were carried out, which gave no evidence for the

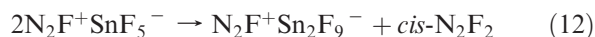
Table 4. Vibrational Spectra of $\text{N}_2\text{F}^+\text{Sn}_2\text{F}_9^-$ Showing the Variation of the Bands from Sample to Sample (Samples A–C) and of a Sample of Mainly $\text{N}_2\text{F}^+\text{SnF}_5^-$ Decomposing to $\text{N}_2\text{F}^+\text{Sn}_2\text{F}_9^-$ and *cis*- N_2F_2 (Sample D)

observed freq, rel int				assignments				
Ra (A)	Ra (B)	Ra (C)	Ra (D) ^a	IR (A)	IR (D) ^a	CCSD(T)/aVTZ ^d	N_2F^+ ($C_{\infty v}$)	anion
2399 [0+]	2384 [1]	2382 [0.5]	2378 [2]	2392 vw	2389 vw	2370.6(2389.4)	$\nu_3 (\Sigma^+)$	
2366 [1]								
1075 [2]	1076 [2.5]	1073 [1]		1075 m		1045.3(1027.3)	$\nu_1 (\Sigma^+)$	
1061 [4]	1060 [5]	1060 [3.5]	1059 [7]	1063 ms	1057 m		$2 \nu_2 (\Sigma^+)$	
758 [0+]								
646 [10]	646 [8.4]	646 [4]		690 vs	662 s			
630 [3]	630 [4]	630 sh		634 s	616 vs			stretching modes
612 [4]	616 [10]	616 [10]	640 [10]	611 ms				
522 [0.5]	519 [1.3]	518 [1]		590 m				
494 [0.5]	490 sh			550 mw	517 ms			
				494 m				
385 [1.5]	385 [1]	388 [1]	386 [4]		385 mw	408.3(388.8)	$\nu_2 (\pi)$	
376 [2]	376 [1.7]	376 [0.8]						
325 [0.5]								
293 [0.3]								
276 [0.2]								
240 [0.3]			220 [1]					
194 [2]	193 [1.8]	^c						deformation modes
177 [1]								
152 [0.7]								
141 [0+]			121 [2]					
124 [0+]	124 [1]							

^a In addition to the listed bands, the following bands without P and R branches were observed due to free *cis*- N_2F_2 trapped in the solid; Ra: 1526 [0+], 888 [4.3], 340 [2]; IR: 2228 w, 1525 mw, 946 m, 881 m, 730 mw. ^b Spectrum recorded as an AgCl pellet, bands below 400 cm^{-1} were obscured by the AgCl. ^c Not observed due to poor signal-to-noise ratio. ^d CEPA-1 values from ref 49 in parentheses.

formation of stable N_2FSnF_5 or $(\text{N}_2\text{F})_2\text{SnF}_6$ salts, but produced only some $\text{N}_2\text{F}^+\text{Sn}_2\text{F}_9^-$.

Further experimental evidence for the instability of $\text{N}_2\text{F}^+\text{SnF}_5^-$ was obtained in one instance when a product with a composition closer to 1:1 was accidentally obtained from the reaction of excess *cis*- N_2F_2 with SnF_4 in HF solution, when the removal time of unreacted N_2F_2 was shortened and the spectra of the solid product were immediately recorded (Figure 3). These vibrational spectra showed the presence of anion bands resembling more closely those previously observed²⁸ for SnF_5^- in $\text{N}_5^+\text{SnF}_5^-$ and a set of bands due to *cis*- N_2F_2 trapped within the solid (Figure 3). Their frequencies are very close to those of free gaseous *cis*- N_2F_2 ,²⁹ however, the rotational P and R branches, characteristic for the free gas, are missing. This demonstrates that N_2FSnF_5 decomposes at room temperature to $\text{N}_2\text{FSn}_2\text{F}_9$ and *cis*- N_2F_2 (eq 12).



The Sn_2F_9^- anion most likely does not have a monomeric structure. Because tin prefers a coordination number of 6 toward fluorine, a monomeric anion would require three fluorine bridges, that is, the sharing of a common face. On the basis of the similarity of the coordination chemistry of Sn(IV) and Ti(IV) and the failure, despite intensive efforts of Mazej and Goreshnik,⁶⁴ to find the corresponding triply bridged monomeric Ti_2F_9^- anion, its existence in tin chemistry is equally unlikely. Depending on the counterion, only either tetrameric, pseudotetrahedral $\text{Ti}_4\text{F}_{18}^{2-}$, or polymeric, infinite double chain $(\text{Ti}_2\text{F}_9^-)_n$ anions were found. On the basis of the complexity of our observed vibrational spectra,

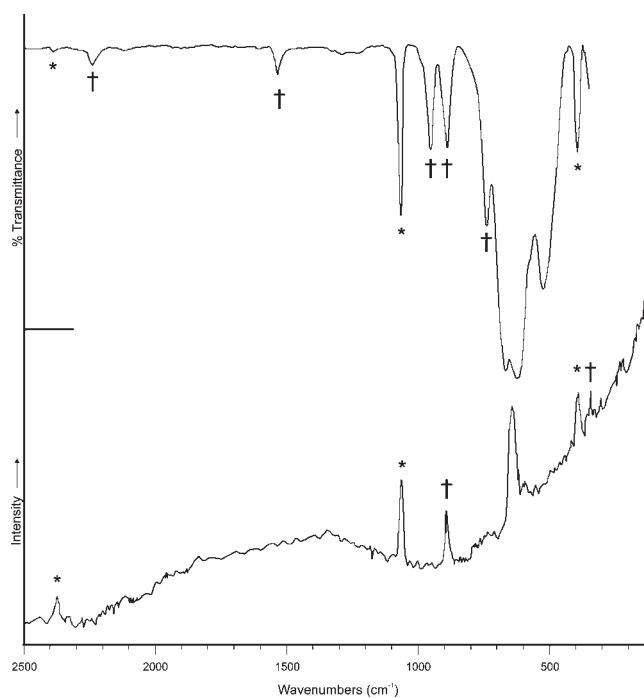


Figure 3. IR (upper trace) and Raman (lower trace) spectra of N_2FSnF_5 undergoing decomposition to $\text{N}_2\text{FSn}_2\text{F}_9$ and *cis*- N_2F_2 . The bands marked by an asterisk are due to N_2F^+ , bands marked by a dagger are due to *cis*- N_2F_2 , and the remaining bands are due to the anion.

the analogy with the titanium system, and our previous findings for SnF_5^- , it is very likely that Sn_2F_9^- is also present as an oligomer or polymer.

Computational Results. Since precise experimental measurements of some of the thermodynamic properties of N_2F_2 and its isomerization process are very difficult

Table 5. Optimized Bond Lengths (Å) and Bond Angles (deg)

molecule	method	R_{NF}	R_{NN}	$\angle \text{FNN}$
<i>cis</i> -N ₂ F ₂ (¹ A ₁ , C _{2v})	CCSD(T)/aVTZ	1.3872	1.2248	114.2
	electron diffraction ⁶³	1.410 ± 0.009	1.214 ± 0.008	114.4 ± 1.0
	microwave ⁶⁴	1.384 ± 0.010	1.214 ± 0.005	114.5 ± 0.5
<i>trans</i> -N ₂ F ₂ (¹ A _g , C _{2h})	CCSD(T)/aVTZ	1.3860	1.2321	104.7
	electron diffraction ⁶³	1.396 ± 0.008	1.231 ± 0.010	105.5 ± 0.7
	CCSD(T)/aVDZ	2.7323	1.1206	180
N ₂ F FNNF(TS)	CCSD(T)/aVTZ	1.7169	1.1521	108.0
		1.2957		171.3
		1.4014	1.3194	107.7 ^a
F ₂ NN	CCSD(T)/aVTZ	1.4409	1.1306	131.3

^a FNNF dihedral angle = 89.8°.

due to its high reactivity and the small differences in the values between the two isomers, high-level electronic structure calculations can provide better values than experiment. A previous molecular orbital study by Lee and co-workers showed⁴ that the calculated values strongly depend on the level of correlation treatment and the basis set. It was, therefore, desirable to perform these calculations at the highest available level.

The calculated CCSD(T)/aVTZ value (Table 3) for the $r_{\text{N}=\text{N}}$ distance in N₂F⁺ is larger by 0.021 Å when compared to the experimental gas phase structure⁵² and $r_{\text{N}-\text{F}}$ is shorter than experiment by 0.010 Å. The calculated r_e of N₂ (¹Σ_g⁺) is 1.104 Å at this level⁶⁵ compared to the experimental value⁶⁶ of 1.0977 Å, a variation of 0.006 Å. The calculated CEPA-1/[8,4,2,1] values⁵² of $r_{\text{N}=\text{N}} = 1.1040$ Å and $r_{\text{N}-\text{F}} = 1.2521$ Å for N₂F⁺ are in somewhat better agreement with experiment than the CCSD(T)/aVTZ values. The anharmonic vibrational frequencies of N₂F⁺, reported⁹ previously as well as in the current work, are in excellent agreement with the calculated CCSD(T)/aVTZ harmonic frequencies (Table 4). The largest difference was found for the F–N=N bend (π mode), which was calculated to be 20 cm⁻¹ higher than the experimental value. Our calculated harmonic frequencies are also within about 20 cm⁻¹ of the anharmonic CEPA-1 values.⁵²

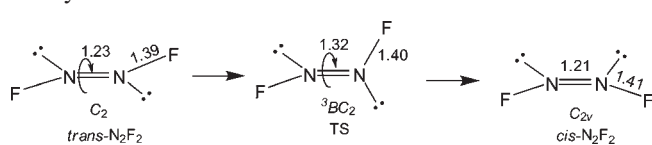
The experimental geometries of *cis*- and *trans*-N₂F₂ have been reported from electron diffraction (*cis* and *trans*)⁶⁷ and microwave spectroscopy (*cis*)⁶⁸ studies. Our CCSD(T)/aVTZ values for *cis*-N₂F₂ are in good agreement with the microwave structure⁶⁸ with the calculated $r_{\text{N}=\text{N}}$ and $r_{\text{N}-\text{F}}$ distances being 0.011 and 0.003 Å, respectively, longer than the experimental values (Table 5). Our CCSD(T)/aVTZ values for *cis*- and *trans*-N₂F₂ are also in good agreement with the electron diffraction structures,⁶⁷ with the predicted $r_{\text{N}-\text{F}}$ distances of both isomers being shorter than the experimental values. Comparison of the microwave and electron diffraction structures suggests that the electron diffraction $r_{\text{N}-\text{F}}$ distances are too long. The calculations do reproduce the electron diffraction difference for the N–N bond lengths in the two isomers but not the difference in the N–F bond lengths. The substantial change in the $\angle \text{FNN}$ for the *cis*- and *trans*-isomers of about 10° is reproduced by

the calculations. The anharmonic vibrational frequencies of *cis*-N₂F₂ and *trans*-N₂F₂ have also been reported^{69,70} and agree well with our calculated CCSD(T)/aVTZ harmonic frequencies, with the largest deviation of 32 cm⁻¹ found for the highest frequency a₁ mode of *cis*-N₂F₂ (Table 6).

The calculated heats of formation are given in Table 7. The components for the atomization energies are given in the Supporting Information. It is predicted that *cis*-N₂F₂ is more stable than *trans*-N₂F₂ by 1.4 kcal/mol at 298 K, consistent with other calculated values⁴ and the experimental equilibrium measurements of Pankratov and Sokolov, who found that within experimental error this value was close to zero.⁴⁸ It should be noted that the current calculations are the most reliable values reported so far. Our calculated heat of formation of the less stable *trans*-N₂F₂ is within 0.1 kcal/mol of the reported experimental value.⁴³ However, our calculated value for *cis*-N₂F₂ is 1.7 kcal/mol higher than the reported experimental value,⁴⁷ due to the smaller calculated energy of isomerization.

In contrast to the small energy difference between the *cis*- and the *trans*-isomers, which also represents the heat of isomerization, the activation energy barriers for the uncatalyzed isomerization of the free molecule are very high, involving transition states that, depending on the isomerization mechanism and the level and basis set used for the calculation, are at least 60 kcal/mol above the ground state. Two different mechanisms can be envisioned for the uncatalyzed *trans*–*cis* isomerization.

The first mechanism involves rotation about the N=N double bond, resulting in a transition state of C₂ symmetry.



The calculated ³B C₂ minimum energy structure with a dihedral F–N–N–F angle of 89.8° (Table 6) lies 59.6 kcal/mol above the *cis*-isomer at 0 K. This represents the lower limit to the isomerization barrier on the singlet surface. The value of ~60 kcal/mol for rotation about the N=N bond is consistent with the value expected for the C=C π -bond.⁷¹

(65) Matus, M. H.; Arduengo, A. J., III; Dixon, D. A. *J. Phys. Chem. A* **2006**, *110*, 10116.

(66) Huber, K. P.; Herzberg, G. Constants of Diatomic Molecules. *Molecular Spectra and Molecular Structure*; Van Nostrand: Princeton, 1979; Vol. IV.

(67) Bohn, R. K.; Bauer, S. H. *Inorg. Chem.* **1967**, *6*, 309.

(68) Kuczkowski, R. L.; Wilson, E. B., Jr. *J. Chem. Phys.* **1963**, *39*, 1030.

(69) Shimanouchi, T. *J. Phys. Chem. Ref. Data* **1977**, *6*, 993.

(70) King, S. T.; Overend, J. *Spectrochim. Acta* **1966**, *22A*, 689.

(71) Nguyen, M. T.; Matus, M. H.; Lester, W. A., Jr.; Dixon, D. A. *J. Phys. Chem. A* **2008**, *112*, 2082.

Table 6. Calculated Vibrational Frequencies (cm⁻¹) at the CCSD(T)/aVTZ Level

molecule	method	symm	calcd	exptl
<i>cis</i> -N ₂ F ₂ (¹ A ₁ , C _{2v})	CCSD(T)	a ₁	1557.3	1525 ^a
		a ₁	920.1	896
		a ₁	345.2	341
		b ₂	967.5	952
		b ₂	750.4	737
<i>trans</i> -N ₂ F ₂ (¹ A _g , C _{2h}) ^a	CCSD(T)	a ₂	551.0	550
		a _g	1549.8	1523 ^b
		a _g	1032.9	1018
		a _g	609.1	603
		a _u	363.5	364
		b _u	1006.7	991
TS-N ₂ F ₂ (¹ A', C _s)	CCSD(T)	b _u	421.1	423
		a'	2116.6	
		a'	961.5	
		a'	499.6	
		a'	304.1	
		a'	882.9i	
		a''	163.8	
N ₂ F ₂ (³ B, C ₂)	CCSD(T)	a	951.4	
		a	719.0	
		a	464.5	
		a	208.2	
		b	809.6	
		b	534.8	
F ₂ N=N (¹ A ₁ , C _{2v}) ^b	CCSD(T)	a ₁	2058.9	
		a ₁	660.0	
		a ₁	498.5	
		b ₁	528.2	
		b ₂	713.4	
		b ₂	418.2	

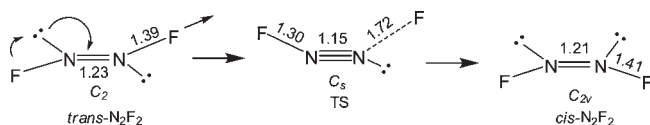
^a Experimental values from ref 29. ^b Experimental values from ref 70.

Table 7. Heats of Formation (kcal/mol) at 0 and 298 K

molecule	$\Delta H_f(0\text{ K})_{\text{theory}}$	$\Delta H_f(298\text{ K})_{\text{theory}}$	$\Delta H_f(298\text{ K})_{\text{expt}}^a$
N ₂	0.8	0.8	0.0
N ₂ F (² Σ _g , C _{∞v})	19.1	19.5	
N ₂ F ⁺ (¹ Σ _g , C _{∞v})	291.2	290.6	
<i>cis</i> -N ₂ F ₂ (¹ A ₁ , C _{2v})	19.5	18.1	16.4
<i>trans</i> -N ₂ F ₂ (¹ A _g , C _{2h})	20.8	19.5	19.4
TS-N ₂ F ₂ (¹ A', C _s)	87.8	86.8	
TS-N ₂ F ₂ (³ B, C ₂)	79.1	78.0	
F ₂ N=N (¹ A ₁ , C _{2v})	33.5	32.4	

^a Reference 43.

The second mechanism involves the in-plane inversion of one fluorine ligand with a transition state of C_s symmetry.



It has a structure similar to that of the N₂F⁺ cation with a significantly shortened N–F bond of 1.30 Å, a very short N–N bond of 1.15 Å, and an F–N–N angle of 170°. The second N–F bond is elongated to 1.72 Å. This transition state has an imaginary frequency of 883i cm⁻¹ and lies 68.7 kcal/mol above the ground state. Thus, contrary to our previous speculation,⁹ the mechanism involving rotation about the N–N bond is energetically favored over the in-plane rearrangement of fluorine ligands, just as in an olefin with a comparable double bond.

Our high-level calculations for the isomerization barriers of the free N₂F₂ molecule are not expected to be in

error by more than 1 to 2 kcal/mol and provide convincing evidence that the barrier is at least 60 kcal/mol. This result is in contrast to the previous CISD and CCSD calculations,⁴ which are too high by up to 20 kcal/mol, and the shock tube measurements,⁷ which reported an experimental barrier of 32 kcal/mol for this process. This latter value is probably highly inaccurate,⁸ considering the great technical difficulties involved in making such a measurement for thermally labile molecules, and should be disregarded. This type of error is consistent with those found in similar shock tube experiments. This explanation is supported by an analysis of the bond dissociation energies in N₂F₂. The N₂F radical is barely stable with respect to loss of an F atom, so N₂F₂ will lose the second F atom as soon as the first N–F bond is broken. The energy for the reaction *cis*-N₂F₂ → N₂ + 2F is only 18.2 kcal/mol at 0 K. Hence, it is possible that isomerization was also occurring by a dissociation/association process. An FN=NF double bond dissociation is highly unlikely because its energy, defined by the reaction N₂F₂ → 2NF, is 93 kcal/mol at 0 K, using $\Delta H_f(\text{NF}) = 55.6$ kcal/mol.⁷² This value is substantially higher than the C=C bond dissociation energy in C₂F₄, defined by the reaction C₂F₄ → 2¹CF₂, which is 68 kcal/mol.⁷³ In view of the relatively low thermal stability of N₂F₂ and the high barriers for the uncatalyzed isomerizations, the uncatalyzed isomerizations of *trans*-N₂F₂ are of lesser practical interest.

The F⁺ affinity of N₂ (calculated using the experimental value⁴⁷ of $\Delta H_{f,0\text{K}}(\text{F}^+) = 419.40$ kcal/mol) is 127 kcal/mol at 0 K and falls in the lower range of the Christe/Dixon oxidizer strength scale⁷⁴ with values that are bracketed by those of OF₂ (122 kcal/mol) and BrF₃O (131 kcal/mol). This confirms the experimental observations that N₂F⁺ is a very powerful oxidative fluorinator.

Contrary to our previous conclusion that Lewis acids do not catalyze the isomerization,⁹ the results from the present study prove that strong Lewis acids do indeed catalyze this process. The catalytic effect of the Lewis acids can be readily understood by the similarity of the C_s transition-state structure of the uncatalyzed isomerization to that of the N₂F⁺ cation. The interaction of *trans*-N₂F₂ with a strong Lewis acid is likely to stretch one N–F bond, while at the same time shortening the other N–F bond as well as the N–N bond and increasing their F–N–N angle. This interaction greatly reduces the energy required for reaching the C_s transition state. It is also easy to understand that increasing Lewis acidity strength^{62,63} lowers the barrier and the required isomerization temperature. Therefore, both *cis*-N₂F₂ and *trans*-N₂F₂ can react with strong Lewis acids to give N₂F⁺ salts. The only difference is that the *cis*-isomer is more reactive. This increased reactivity of the *cis*-isomer can be readily explained. In both N₂F₂ isomers, each nitrogen atom possesses a sterically active free valence electron pair. The transformation of N₂F₂ to N₂F⁺ requires the conversion of the N=N double bond into a N≡N triple bond by an overlap of electrons from these two free valence

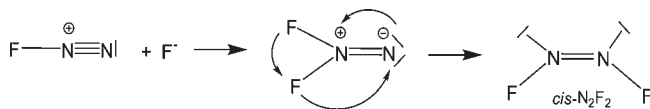
(72) Feller, D.; Peterson, K. A.; Dixon, D. A. *J. Chem. Phys.* **2008**, *129*, 204015.

(73) Dixon, D. A.; Feller, D.; Sandrone, G. *J. Phys. Chem. A* **1999**, *103*, 4744.

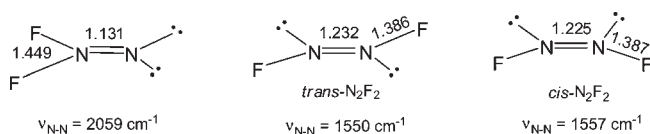
(74) Christe, K. O.; Dixon, D. A. *J. Am. Chem. Soc.* **1992**, *114*, 2978.

electron pairs. Obviously, this overlap is greatly facilitated in *cis*-N₂F₂, where these free pairs are on the same side of the molecule.

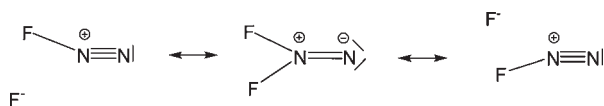
Another characteristic of the N₂F₂ reaction chemistry is the exclusive formation of *cis*-N₂F₂ when N₂F⁺ reacts with F⁻ (eq 4). Why is it that the typical 9:1 mol ratio of *cis*-N₂F₂ to *trans*-N₂F₂ is not obtained, which is experimentally observed for the *trans*-*cis* isomerization reactions? This feature can be readily explained by the charge distribution in N₂F⁺. The central N atom carries the formal positive charge and, therefore, F⁻ attacks exclusively the central N atom, generating an F₂NN intermediate, which rearranges itself by an in-plane α -fluorine migration to *cis*-N₂F₂.



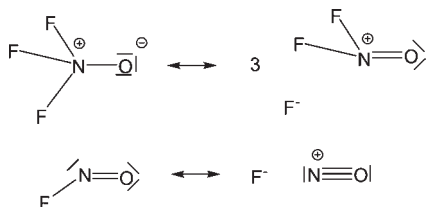
Because of the involvement of the F₂N=N isomer in this reaction, it was interesting to explore this isomer in more detail. It lies 14.3 kcal/mol above the *cis*-isomer at 298 K, explaining its tendency to rearrange to the energetically favored *cis*-N₂F₂. Its calculated geometry and vibrational spectra are given in Tables 5 and 6, respectively. No experimental data are known for this isomer, and the spectrum originally attributed⁷⁵ to F₂N=N by Sanborn is that of *cis*-N₂F₂.³ Compared to *cis*-N₂F₂ and *trans*-N₂F₂, the calculated N–N bond length in F₂N=N is dramatically shortened by about 0.10 Å, while the N–F bond lengths are increased by about 0.06 Å.



Similarly, the N–N stretching frequency is increased by about 500 cm⁻¹, while the NF₂ stretching frequencies are decreased by an average of about 300 cm⁻¹, indicating that in F₂N=N strong contributions from the following resonance structures must be invoked to describe its bonding appropriately.



This strong contribution from highly polar N–F bonds resembles those encountered for F₃NO¹⁰ and FNO.^{11,12}



The driving force behind these highly unusual resonance structures for nitrogen fluorides and oxofluorides is the

desire of fluorine, which is more electronegative than oxygen or nitrogen, to carry the negative charges.

Conclusions

The present work describes improved methods for the synthesis of N₂F⁺ salts, which are the key precursors to novel high energy density materials, such as N₅⁺ salts. Important improvements include the use of cheap natural graphite flakes in place of expensive highly oriented pyrolytic graphite (HOPG) for the preparation of the first-stage graphite-AsF₅ intercalate and of better catalysts for the N₂F₂ *trans*-*cis* isomerization, the elimination of extra reaction steps, and significant reductions in the reaction times required for the synthesis of N₂F⁺ salts, from several weeks to several days. Also, the first ordered crystal structure of an N₂F⁺ salt was obtained, thus providing individual N≡N and N–F bond lengths for a direct comparison with the free molecule. These bonds are among the shortest experimentally observed N≡N and N–F bond lengths. Furthermore, the new N₂F⁺ salt, N₂F⁺Sb₂F₉⁻, has been synthesized and characterized. High-level correlated molecular calculations were carried out and show that *cis*-N₂F₂ is more stable than *trans*-N₂F₂ by 1.4 kcal/mol at 298 K. In addition, the calculations demonstrate that the lowest energy uncatalyzed isomerization pathway involves rotation about the N=N double bond and has a barrier of 60 kcal/mol. This rotation barrier is substantially above the energy required for the dissociation of N₂F₂ to N₂ and 2F. Therefore, some of the N₂F₂ can dissociate before undergoing uncatalyzed isomerization, resulting in autocatalysis by the decomposition products. It is shown that the *trans*-*cis* isomerization of N₂F₂ is catalyzed by strong Lewis acids, most likely involves a planar transition state of symmetry C_s, and yields a 9:1 equilibrium mixture of *cis*-N₂F₂ and *trans*-N₂F₂. Explanations are given for the increased reactivity of *cis*-N₂F₂ with Lewis acids and the exclusive formation of *cis*-N₂F₂ in the reaction of N₂F⁺ with F⁻. The geometry and vibrational frequencies of the F₂N=N isomer have also been calculated and imply strong contributions from ionic N₂F⁺ F⁻ resonance structures.

Acknowledgment. We gratefully acknowledge financial support of this work by the Air Force Office of Scientific Research, DARPA, the Office of Naval Research, the National Science Foundation, and the Department of Energy. D.A.D. is indebted to the Robert Ramsay Endowment of the University of Alabama.

Supporting Information Available: Crystal data and structure refinement for N₂F⁺SbF₆⁻ (Table S1); atomic coordinates ($\times 10^4$) and equivalent isotropic displacement parameters ($\text{Å}^2 \times 10^3$) for N₂F⁺SbF₆⁻ (Table S2); bond lengths and angles for N₂F⁺SbF₆⁻ (Table S3); atomic coordinates ($\times 10^4$) and equivalent isotropic displacement parameters ($\text{Å}^2 \times 10^3$) for N₂F⁺Sb₂F₁₁⁻ (Table S4); CCSD(T)/aVnZ total energies (E_h) as a function of the basis set (Table S5); components for calculated atomization and reaction energies in kcal/mol (Table S6); ORTEP plot for N₂F⁺SbF₆⁻ with thermal ellipsoids at the 30% probability level (Figure S1); packing diagram of N₂F⁺SbF₆⁻ along the *c*-axis (Figure S2); packing diagram of N₂F⁺Sb₂F₁₁⁻ along the *a*-axis (Figure S3); IR and Raman spectra of N₂FSn₂F₉ (Figure S4); and X-ray crystallographic file in CIF format for the structure determinations of N₂FSbF₆ and N₂FSb₂F₁₁. This material is available free of charge via the Internet at <http://pubs.acs.org>.

(75) Sanborn, R. H. *J. Chem. Phys.* **1960**, *33*, 1855.